Functionalized Silicone Nanospheres: Synthesis, Transition Metal Immobilization, and Catalytic Applications

Christopher A. Bradley, Benjamin D. Yuhas, Meredith J. McMurdo, and T. Don Tilley*

Department of Chemistry, University of California at Berkeley, Berkeley, California 94720, and the Chemical Sciences Division, Lawrence Berkeley National Laboratory, 1 Cyclotron Road, Berkeley, California 94720

Received July 3, 2008. Revised Manuscript Received September 9, 2008

Silicone nanospheres containing a variety of functional groups (pyridines, phosphines, thiols, amines, etc.) have been prepared by emulsion copolymerization of methyltrimethoxysilane, $MeSi(OMe)_3$, and the functionalized monomer of interest, $RSi(OMe)_3$. This procedure provides a reproducible synthesis of spherical particles in the 12−28 nm size regime as determined by transmission electron microscopy (TEM). The presence of the functional groups is supported by a combination of spectroscopic methods including DRUV−vis, DRIFTS, and NMR spectroscopy. Comonomer dispersity within the nanospheres was probed using elemental mapping techniques, and these support a homogeneous distribution of functional groups within the particles. Palladium(0) immobilization on phosphine-substituted nanospheres also results in a random distribution of the transition metal throughout the particles. Nanospheres containing multiple acid/base functionalities were also prepared, and these demonstrate functional group cooperativity based on enhanced conversions in the base-catalyzed Henry reaction, relative to nanosphere catalysts containing only basic groups. The diversity of functional groups that may be incorporated into the spheres suggests that these materials hold considerable promise as ligand supports and catalysts.

Introduction

Silicone- or siloxane-based materials serve as useful supports for a variety of reaction centers, including those based on organic functional groups and transition metals.[1,2] Depending upon the conditions of synthesis or the type of templating agents employed, a range of shapes and length scales can be accessed for silicone-based particles.[3,4] Silicone nanomaterials are gaining increasing attention, given their inherent robustness and their tunable physical properties.[5−8] Thus, these materials are being considered for a diverse range of applications, including drug delivery[9,10] as well as ligand[11] or catalyst[12] supports. For these reasons, the development of new and versatile synthetic routes to functionalized silicone nanomaterials, having well-defined shape and size distributions, is highly desirable.

Current strategies for incorporation of functionality into silicone materials rely heavily on condensation of substituted alkoxysilanes onto preformed supports[13] or of tetraethylorthosilicate (TEOS) with a silane monomer containing the desired functional group, to give copolymer networks.[14,15] Using these strategies, materials containing simple functionalities, such as thiol and amine groups, are accessible, but the templating methods used to prepare the particles usually

* Corresponding author. E-mail: tdtilley@berkeley.edu.

(1) (a) Clarson, S. J.; Fitzgerald, J. J.; Owen, M. J.; Smith, S. D.; Van Dyke, M. E. *Synthesis and Properties of Silicones and Silicone-Modified Materials*; ACS Symposium Series 838; American Chemical Society: Washington, DC, 2003. (b) Clarson, S. J.; Fitzgerald, J. J.; Owen, M. J.; Smith, S. D.; Van Dyke, M. E. *Science and Technology of Silicones and Silicone-Modified Materials*; ACS Symposium Series 964; American Chemical Society: Washington, DC, 2007. (c) Sanchez, C.; Ribot, F.; Lebeau, B. *J. Mater. Chem.* **1999**, *9*, 35.

(2) For recent examples of siloxane particles as catalyst supports, see (a) Soga, K.; Arai, T.; Hoang, B.; Uozami, T. *Macromol. Rapid Commun.* **1995**, *16*, 905. (b) Koppel, A.; Alt, H. G.; Schmidt, R. *J. Organomet. Chem.* **1999**, *577*, 351. (c) Schmidt, R.; Alt, H. G.; Ebenhoch, J. *J. Appl. Polym. Sci.* **2001**, *80*, 281. (d) Schmidt, R.; Alt, H. G.; Ebenhoch, J. *J. Appl. Polym. Sci.* **2001**, *80*, 613.

(3) For silicone nanospheres, see (a) Jungmann, N.; Schmidt, M.; Maskos, M. *Macromolecules* **2001**, *34*, 8347. (b) Baumann, F.; Deubzer, B.; Geck, M.; Dauth, J.; Schmidt, M. *Macromolecules* **1997**, *30*, 7568.

(4) For silicone nanorods, see Pol, V. G.; Pol, S. V.; Gedanken, A.; Lim, S. H.; Zhong, Z.; Lin, J. *J. Phys. Chem. B* **2006**, *110*, 11237.

(5) For recent work with core−shell siloxane particles, see (a) Jungmann, N.; Schmidt, M.; Maskos, M. *Macromolecules* **2002**, *35*, 6851. (b) Nakade, M.; Ikeda, T.; Ogawa, M. *J. Mater. Sci.* **2007**, *42*, 4815. (c) Graf, C.; Schärtl, W.; Fischer, K.; Hugenberg, N.; Schmidt, M. *Langmuir* **1999**, *15*, 6170.

(6) For a recent example of hollow siloxane nanocapsules, see Wang, H.; Chen, P.; Zheng, X. *J. Mater. Chem.* **2004**, *14*, 1648.

(7) For luminescent siloxane containing materials, see (a) Fernandes, M.; de Zea Bermudez, V.; Sá Ferreira, R. A.; Carlos, L. D.; Charas, A.; Morgado, J.; Silva, M. M.; Smith, M. J. *Chem. Mater.* **2007**, *19*, 3892. (b) Koslova, N. I.; Viana, B.; Sanchez, C. *J. Mater. Chem.* **1993**, *3*, 111. (c) Zou, J.; Baldwin, R. K.; Pettigrew, K. A.; Kauzlarich, S. M. *Nano Lett.* **2004**, *4*, 1181.

(8) For an example of surface area effects on enhanced As remediation using Fe_3O_4 nanoparticles, see Yavuz, C. T.; Mayo, J. T.; Yu, W. W.; Prakash, A.; Falkner, J. C.; Yean, S.; Cong, L.; Shipley, H. J.; Kan, A.; Tomson, M.; Natelson, D.; Colvin, V. L. *Science* **2006**, *314*, 964.

(9) Kepczynski, M.; Lewandowska, J.; Romek, M.; Zapotoczny, S.; Ganachaud, F.; Nowakowska, M. *Langmuir* **2007**, *23*, 7314.

(10) Kim, H.-Y.; Matsuda, H.; Zhou, H.; Honma, I. *Adv. Mater.* **2006**, *18*, 3083.

(11) For a general review of polymer catalyst supports, see Leadbeater, N. E.; Marco, M. *Chem. Rev.* **2002**, *102*, 3217.

(12) Bonnette, F.; Kato, F.; Destarac, M.; Mignani, G.; Cossío, F. P.; Baceiredo, A. *Angew. Chem., Int. Ed.* **2007**, *46*, 8632.

(13) (a) Tanaka, K.; Shinoda, S.; Takai, N.; Takahashi, H.; Saito, Y. *Bull. Chem. Soc. Jpn.* **1980**, *53*, 1242. (b) Elings, J. A.; Ait-Medour, R.; Clark, J. H.; Macquarrie, D. J. *Chem. Commun.* **1998**, 2707. (c) Kidder, M. K.; Britt, P. F.; Zhang, Z.; Dai, S.; Hagaman, E. W.; Chaffee, A. L.; Buchanan, A. C., III. *J. Am. Chem. Soc.* **2005**, *127*, 6353. (d) Alauzun, J.; Mehdi, A.; Reye, C.; Corriu, R. J. P. *J. Am. Chem. Soc.* **2006**, *128*, 8718.

(14) Burns, A.; Ow, H.; Wiesner, U. *Chem. Soc. Rev.* **2006**, *35*, 1028.

10.1021/cm8018154 CCC: $40.75
Published on Web 12/11/2008

limit particle size to nanospheres with diameters of >100 nm. The challenge remains to develop simple, general procedures for the preparation of well-defined, functionalized silicone nanomaterials, particularly with dimensions below 100 nm.

The work reported here was motivated by an interest in organic soluble, silicone nanospheres for use as macromolecular catalyst supports. Such materials may contain single site active centers amenable to solution and solid state characterization techniques. Using methods similar to those reported for generation of unfunctionalized silicone nanospheres,[16] we obtained 14−20 nm silicone nanospheres functionalized with silanol groups. The latter materials possess high surface areas, are hydrophobic, and have been used as supports for titanium centers that catalyze the selective epoxidation of cyclohexene (eq 1).[17] Given these results, it is clear that silicone nanospheres represent promising catalyst supports that may offer solubility and tailored chemical environments for the catalyst centers. However, a more general utilization of this approach requires development of reliable synthetic procedures that allow incorporation of a diverse array of functional groups (phosphines, thiols, amines, etc.) onto the silicone nanospheres.

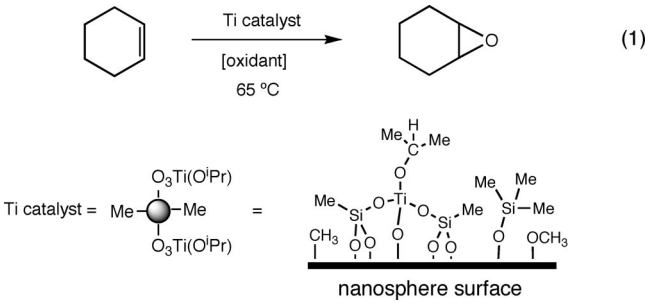

This report describes a modular procedure for the synthesis of functionalized silicone nanospheres. These procedures are based on a copolymerization of methyltrimethoxysilane with a substituted silane of interest (eq 2). Several monomers appear amenable to this copolymerization method, and a wide range of comonomer loadings are possible. On the basis of elemental mapping techniques, the functional groups appear well dispersed throughout the nanoparticles. In addition, more complex nanospheres were prepared, via introduction of amine and ureido groups into the nanospheres. These groups appear to be well dispersed in the nanospheres, indicated by their cooperative participation during nitroaldol catalysis.

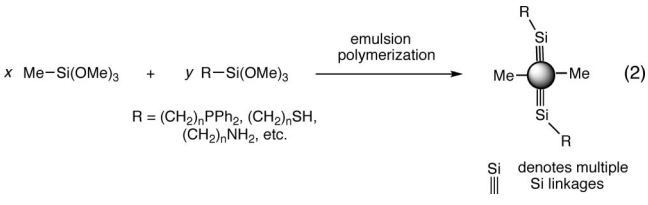

Experimental Section[18]

General Information. All air- and moisture-sensitive manipulations were carried out using standard Schlenk and cannula techniques or in a Vacuum Atmospheres inert atmosphere drybox containing an atmosphere of purified nitrogen. Solvents for air- and moisture sensitive manipulations were initially dried and deoxygenated using literature procedures.[19] Benzene-d_6 (Cambridge Isotopes) for NMR spectroscopy was distilled from sodium metal under an atmosphere of nitrogen prior to use. Chloroform-*d* (Cambridge Isotopes) was dried over sieves prior to use. Methyltrimethoxysilane, vinyltrimethoxysilane, and hexamethyldisilazane were obtained from Wacker Chemie and used as received. Methoxytrimethylsilane, 4-vinyl pyridine, azobisisobutyronitrile (AIBN), diphenylphosphine, sodium iodide, sodium azide, *n*-butyl lithium (1.6 M in hexanes), (3-chloropropyl)trimethoxysilane, Ellman's reagent, phenol, nitromethane, 4-nitrobenzaldehyde, and ninhydrin were purchased from Aldrich and used as received. 2-[2-(Trimethoxysilyl)ethyl]pyridine, (3-mercaptopropyl)trimethoxysilane, (3-aminopropyl)trimethoxysilane, *N*-(2-aminoethyl)-3-aminopropyltrimethoxysilane, and ureidopropyltrimethoxysilane were purchased from Gelest and used as received. Acetonitrile was purchased from Aldrich and refluxed over P_2O_5 before distillation and use. Tetrahydrofuran was refluxed over sodium prior to distillation and use. Trichlorosilane was purchased from Gelest and distilled prior to use. Triethylamine, tri-iso-propylamine, and dimethylformamide were purchased from Aldrich and stored over sieves prior to use. Indene was purchased from Aldrich and distilled prior to use. Deionized water was stirred for 16 h with charcoal prior to distillation. Tris(dibenzylideneacetone)dipalladium(0) was purchased from Strem and used as received. Benzethonium chloride was purchased from Aldrich and used as received. (Trimethylsilyl)indene,[20] 4-[2-(trimethoxysilyl)ethyl]pyridine,[21] and 2-(diphenylphosphino)ethyltrimethoxysilane[22] were prepared according to literature procedures.

Solution ^{1}H NMR spectra were recorded on a Bruker AVQ-400 spectrometer operating at 400.13247 MHz. Solution ^{13}C NMR spectra were recorded on a Bruker AVQ-400 spectrometer operating at 100.62283 MHz. Solution ^{31}P NMR spectra were recorded on a Bruker AVQ-400 spectrometer operating at 161.96748 MHz. All chemical shifts are reported relative to $SiMe_4$ using residual ^{1}H NMR chemical shifts of the solvent as a secondary standard. Solid state NMR experiments (unless otherwise noted) were performed on a Bruker Avance 500 spectrometer equipped with an 11.75 T magnet and a Bruker 4 mm CPMAS probe with an MAS rate of 14.5 kHz. The ^{1}H MAS NMR spectrum was acquired with a Hahn-echo pulse sequence (90-τ-180-acquisition) with τ being synchronized with rotor time. The 90° pulse width was 2.2 μs, the data size was 32K, the spectrum width was 500 kHz, the relaxation delay was 5 s, and the number of scans was 80. The ^{13}C CPMAS NMR spectra were recorded with a ramped-CP power level and TPPM decoupling technique, with a contact time of 1.5 ms, a relaxation

(15) For representative examples, see (a) Sutra, P.; Brunel, D. *Chem. Commun.* **1996**, 2485. (b) Lim, M. H.; Blanford, C. F.; Stein, A. *J. Am. Chem. Soc.* **1997**, *119*, 4090. (c) Fan, H.; Lu, Y.; Stump, A.; Reed, S. T.; Baer, T.; Schunk, R.; Perez-Luna, V.; Lopez, G. P.; Brinker, C. J. *Nature* **2000**, *40*, 56. (d) Richer, R.; Mercier, L. *Chem. Mater.* **2001**, *13*, 2999. (e) Yang, Q.; Kapoor, M. P.; Inagaki, S. *J. Am. Chem. Soc.* **2002**, *124*, 9694. (f) Huh, S.; Chen, H.-T.; Wiench, J. W.; Pruski, M.; Lin, V. S.-Y. *Chem. Mater.* **2003**, *15*, 4247.
(16) Baumann, F.; Deubzer, B.; Geck, M.; Dauth, J.; Sheiko, S.; Schmidt, M. *Adv. Mater.* **1997**, *9*, 955.
(17) Bradley, C. A.; McMurdo, M. J.; Tilley, T. D. *J. Phys. Chem. C.* **2007**, *111*, 17570.
(18) For additional experimental procedures and details, see the Supporting Information.
(19) Pangborn, A.; Giardello, M.; Grubbs, R. H.; Rosen, R.; Timmers, F. *Organometallics* **1996**, *15*, 1518.
(20) Davison, A.; Rakita, P. E. *J. Organomet. Chem.* **1970**, *23*, 407.
(21) (a) Grüniger, H.-R.; Calzaferri, G. *Helv. Chim. Acta* **1979**, *62*, 2547. (b) Corriu, R. J. P.; Lancelle-Beltran, E.; Mehdi, A.; Reyé, C.; Brandés, S.; Guilard, R. *J. Mater. Chem.* **2002**, *12*, 1355.
(22) Uriarte, R.; Mazanec, T. J.; Tau, K. D.; Meek, D. W. *Inorg. Chem.* **1980**, *19*, 79.

delay of 1.2 s, a spectral width of 100 kHz, a data size of 8K, and 20 000 scans. The chemical shift was referenced to the carboxyl group in glycine at 176 ppm. The ^{29}Si CPMAS NMR spectra were recorded with a Bruker 7 mm CPMAS probe with a zirconia rotor spinning at 5 kHz. The data size was 4K, the number of scans was 14 000, the contact time was 2 ms, and the relaxation time was 1 s. The spectrum was Fourier transformed with 80 Hz line broadening. A ramp-contact power and TPPM decoupling pulse sequence was used for the experiment. Certain ^{13}C and ^{29}Si (148.87 MHz) spectra were recorded on a Varian Inova 750 MHz spectrometer; these spectra are denoted in the Supporting Information.

Transmission electron microscopy was performed using a Phillips Tecnai 12 instrument at an accelerating voltage of 200 kV. Samples were prepared by dissolution in methylene chloride (3 mL) followed by sonication for 30 min and deposition on carbon-Cu grids or C-flat holey carbon grids (Electron Microscopy Services). The grids were then allowed to air dry overnight prior to analysis. Samples for EDX analysis were prepared in a similar fashion exclusively on holey carbon grids. Energy-dispersive X-ray spectroscopy (EDX) measurements were performed on a Phillips CM200-FEG transmission electron microscope operating at 200 kV. The spot size for each spectral acquisition was approximately 18 nm.

Diffuse reflectance UV−visible spectra were acquired using a Labsphere DRA-CA-30I diffuse-reflectance attachment on a Varian-Cary 300 Bio spectrophotometer with a spectral bandwidth of 2 nm and a collection speed of 600 nm/min. A MgO sample was used as a reference material prior to data collection. Solution UV−visible spectra were acquired on the same instrument using similar conditions. DRIFTS spectra were collected on a Nicolet Nexus 6700 FTIR spectrometer with a liquid nitrogen cooled MCT-B detector using a Pike Technologies EasiDiff diffuse-reflectance attachment and a 10 mm diameter sample cell. A total of 512 scans were performed on each sample with a resolution of 4.0 cm^{-1}. KBr was used as the background. IR spectra in a Nujol matrix were acquired on the same instrument with 32 scans per sample. Thermal analyses (TGA/DSC) were performed on a TA Instruments SDT 2960 Integrated TGA/DSC analyzer with a heating rate of 10 °C/min under a flow of nitrogen or oxygen.

Nitrogen adsorption isotherms were collected at 77 K on a Quantachrome Autosorb 1 instrument. Samples were outgassed at 150 °C for 12 h prior to measurement. For all isotherms, warm and cold free space correction measurements were performed with ultrahigh purity He gas (99.999%). Elemental analyses were performed by the College of Chemistry microanalytical laboratory at the University of California, Berkeley, or by Galbraith Laboratories (Knoxville, TN).

Preparation of (3-[(Trimethylsilyl)indenyl]propyl)trimethoxysilane. Trimethylsilylindene (6.05 g, 32 mmol) in a Schlenk flask was dissolved in 200 mL of THF, and the resulting solution was cooled to −78 °C under dinitrogen. To this solution, 21 mL (34 mmol) of 1.6 M *n*BuLi was added and the reaction mixture was warmed to ambient temperature. Upon stirring for 6 h, the solution containing the in situ generated lithium salt was cooled to −78 °C, and 9.28 g (32 mmol) of (3-iodopropyl)trimethoxysilane was added. Upon warming to ambient temperature, the reaction was stirred for an additional 12 h. Solvent removal under vacuum followed by extraction with hexanes and filtration through celite gave a light orange/yellow solution. Subsequent solvent removal under vacuum gives 7.40 g (66%) of an orange oil, identified as pure (3-[(trimethylsilyl)indenyl]propyl)trimethoxysilane by ^{1}H NMR spectroscopy. ^{1}H NMR ($CDCl_3$): $\delta = -0.07$ (s, 9H, Si*Me*$_3$), 0.77 (t, 8 Hz, 2H, C*H*$_2$), 1.82 (m, 2H, C*H*$_2$), 2.64 (m, 2H, C*H*$_2$), 3.36 (br, 1H, C*H*), 3.56 (s, 9H, O*Me*), 6.30 (s, 1H, C═C*H*), 7.16 (t, 8 Hz, 1H, Ind), 7.24 (t, 8 Hz, 1H, Ind), 7.40 (d, 8 Hz, 2H, Ind). ^{13}C NMR ($CDCl_3$): $\delta = -2.23$ (Si*Me*$_3$), 9.45, 22.05, 31.22 (*C*H$_2$), 44.70 (*C*H), 50.74 (O*Me*), 119.16, 122.95, 123.69, 124.66, 130.30, 141.52, 144.63, 146.34 (Ind). MS: 350 (M+). UV−vis (CH_3CN, nm): 254 ($\pi-\pi^*$).

Representative Synthetic Procedure for Functionalized Nanospheres ($NS_{4\text{-py}}$(9:1)). The spheres were prepared by a modified literature procedure.[17] A 250 mL Schlenk flask was charged with benzethonium chloride (0.384 g, 0.86 mmol) and NaOH (0.005 g, 0.13 mmol). Deionized water (100 mL) was added, and the solution was stirred vigorously for 5 min. Methyltrimethoxysilane (4.5 g, 33.0 mmol) and 4-[2-(trimethoxysilyl)ethyl]pyridine (0.5 g, 2.2 mmol) were then added dropwise over the course of 5 min. The emulsion was stirred vigorously for 5 h before methoxytrimethylsilane (1.6 mL, 0.012 mmol) was added to the reaction. After stirring for an additional 12 h, the emulsion was added to methanol (200 mL). Filtration of the corresponding precipitate followed by copious rinsing with methanol gave a colorless powder. (Note: extensive drying of the solid causes sphere aggregation and insolubility.) The material was then transferred to a 100 mL round bottomed flask and dispersed in toluene (60 mL). Hexamethyldisilazane (2.1 mL, 0.010 mmol) was then added, and the solution was stirred for an additional 16 h. The solution was then poured onto methanol (200 mL). Collection of the precipitate on a Büchner funnel followed by drying on a vacuum line gives the nanospheres as a white powder (2.27 g), which may be redispersed in arene or chlorinated organic solvents. Elem anal. Found (%): C, 24.70; H, 5.35; N, 1.06. ^{1}H MAS NMR: $\delta = 0.01$ (Si*Me*), 3.57 (O*Me*), 6.98 (py), 8.38 (py). ^{13}C CPMAS NMR: $\delta = -3.40$ (Si*Me*), 13.99, 28.46 (*C*H$_2$), 49.49 (O*Me*), 123.21, 149.47, 153.20 (py). ^{29}Si CPMAS NMR (750 MHz instrument): $\delta = -66.42$, −57.81, −48.96, (O_3*Si*R), 7.78 (O*Si*Me$_3$). IR (DRIFTS, cm^{-1}): 1610 (C═C, *C*═N), 3071 (sp^2 CH). UV−vis (CH_3CN, nm): 257 ($\pi-\pi^*$).

Synthesis of Palladium-Tethered Nanospheres ($PdNS_{PPh2}$(9:1)). A thick-walled glass vessel was charged with 500 mg of **NS_{PPh2}(9:1)** and 22 mg of (24 mmol, 1 wt% Pd) of $Pd_2(dba)_3$ in a drybox. The vessel was sealed and connected to a Schlenk line, and then 20 mL of toluene was added. The reaction mixture was allowed to stir for 12 h. Solvent was removed under vacuum, and the yellow solid was rinsed five times with 30 mL portions of hexanes. Upon drying the solid under vacuum, 465 mg of **$PdNS_{PPh2}$(9:1)** was isolated as a yellow solid and stored under an inert atmosphere. Elem anal. Found (%): Pd, 0.87. IR (DRIFTS, cm^{-1}): 1577, 1589, 1622, 1643, 1658 (C═C, C═O), 3057, 3078 (sp^2 CH). UV−vis (CH_3CN, nm): 228, 318 ($\pi-\pi^*$).

Representative Procedure for the Nitroaldol Reaction Using Nanosphere Catalysts. A 3 mL vial was charged with 250 mg (1.65 mmol) of 4-nitrobenzaldehyde and the appropriate amount of nanosphere catalyst (either 40 mg of **NS_D(9.5:0.5)**, 40 mg of **NS_D(9.5:0.5)** and 40 mg of **NS_U(9.5:0.5)**, or 40 mg of **NS_{DU}(9:0.5:0.5)**). Nitromethane (3 mL) was then added, and the reaction mixture was heated at 50 °C for 1 h. Solvent was removed under vacuum and a portion of the corresponding solid (10 mg) was dissolved in a 0.01 M ferrocene $CDCl_3$ solution. Integration of the ratio of 4-nitrobenzaldehyde to alkene product gave the percent conversion. Depending on the specific catalyst, these typically ranged between 20−50%. The catalysis was performed 20 times with each catalyst system, and the conversion was averaged over all trials. Performing the catalysis with different batches of the three nanospheres gave similar reproducible conversions.

Results and Discussion

Selection and Synthesis of the Trimethoxysilane Monomers. Monomers were chosen with several design criteria in mind. First, a diverse range of functionalities was

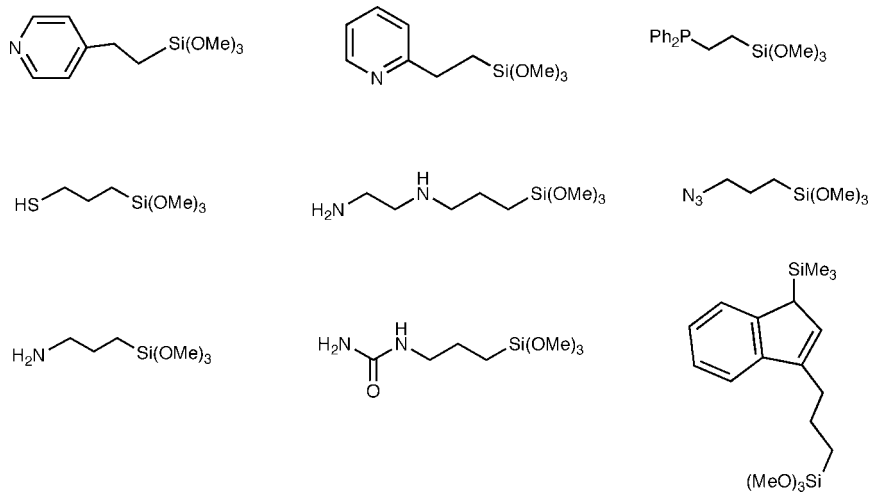

Figure 1. Monomers examined for nanosphere formation.

desired to assist grafting of a variety of transition metal centers. Also, commercial monomers or those prepared in a minimal number of high yielding steps were targeted to facilitate general use of the nanomaterials. Two classes of monomers were investigated: (1) those with a two-carbon spacer between the functional group of interest and the trimethoxysilyl moiety and (2) monomers containing a three-carbon spacer (Figure 1).

Monomers with two-carbon spacers were derived from addition reactions across vinyl groups. For example, 4-[2-(trimethoxysilyl)ethyl]pyridine was synthesized in a two step procedure by hydrosilylation of 4-vinyl pyridine with trichlorosilane to afford the [4-(trichlorosilyl)ethyl]pyridine followed by methanolysis.[21] The phosphine-containing monomer was prepared by light-assisted P−H bond addition to vinyl trimethoxysilane.[22]

^{1}H NMR spectra of the three monomers containing ethylene spacers (in $CDCl_3$) reveal methylene hydrogens in the 0.8−3.0 ppm region while aryl resonances are observed above 7.0 ppm. ^{13}C NMR spectra display resonances in the 10−30 ppm region attributed to the ethylene spacers, while aryl resonances are observed in the 120−160 ppm region. A ^{31}P NMR spectrum of the diphenylphosphine monomer displays a peak at −9.32 ppm, comparable to the ^{31}P signal observed for related aryl phosphines, thus suggesting that the monomer has not undergone oxidation. All monomers display a singlet resonance for the methoxy groups, typically between 3.4−3.6 and 45−60 ppm, in the ^{1}H and ^{13}C NMR spectra, respectively.

Monomers containing a three-carbon spacer were commercially available or were accessed via S_N2 displacements of an iodide leaving group from (3-iodopropyl)trimethoxysilane. Preparation of (3-azidopropyl)trimethoxysilane, a potential synthon for click chemistry on a nanosphere surface,[23] was accomplished by reaction of (3-iodopropyl)-trimethoxysilane with excess sodium azide in DMF.[24] The monomer containing a substituted silyl indene, prepared for the first time in this study, was synthesized by addition of (3-iodopropyl)trimethoxysilane to the lithium indenide salt in THF (eq 3).[25] The silyl indenyl moiety was chosen for the ability of the corresponding anion to mediate unusual changes in hapticity and reactivity of molecular complexes.[26] The trimethylsilyl substituent was used to permit grafting of transition metals via neutral, silyl halide eliminations.[27]

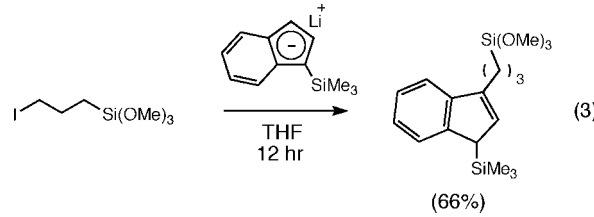

Infrared spectra of selected monomers proved informative and diagnostic for specific functional groups. A Nujol suspension of the azide monomer displays a characteristic stretch of medium intensity at 2097 cm^{-1} while NH stretches are observed for the amine-containing monomers, in the 3400−3500 cm^{-1} range. UV visible spectra of certain monomers also proved diagnostic for the incorporated functionalities. The indenyl and azide monomers each display absorbances at 254 and 278 nm in acetonitrile, corresponding to $\pi-\pi^*$ transitions. The complete characterizations of the functionalized monomers by NMR, IR, and UV−visible spectroscopy proved useful for investigation of their incorporation into nanospheres (vide infra).

(23) For recent representative reviews on click chemistry, see (a) Kolb, H. C.; Finn, M. G.; Sharpless, K. B. *Angew. Chem., Int. Ed.* **2001**, *40*, 2004. (b) Moses, J. E.; Moorhouse, A. D. *Chem. Soc. Rev.* **2007**, *36*, 1249. (c) Nandivada, H.; Jiang, X.; Lahann, J. *Adv. Mater.* **2007**, *19*, 2197.

(24) Verkade, J. G.; Lin, V. S.-Y.; Sarkar, A. U.S. Pat. Appl. Publ. US 2005176978, 2005.

(25) Brady, E. D.; Overby, J. S.; Meredith, M. B.; Mussman, A. B.; Cohn, M. A.; Hanusa, T. P.; Yee, G. T.; Pink, M. *J. Am. Chem. Soc.* **2002**, *124*, 9556.

(26) (a) Bradley, C. A.; Keresztes, I.; Lobkovsky, E.; Young, V. G.; Chirik, P. J. *J. Am. Chem. Soc.* **2004**, *126*, 16937. (b) Bradley, C. A.; Lobkovsky, E.; Keresztes, I.; Chirik, P. J. *J. Am. Chem. Soc.* **2005**, *127*, 10291. (c) Rerek, M. E.; Ji, L. N.; Basolo, F. *J. Chem. Soc., Chem. Commun.* **1983**, *21*, 1208. (d) Alt, H. G.; Schertl, P.; Köppl, A. *J. Organomet. Chem.* **1998**, *568*, 263. (e) Alt, H. G. *Dalton Trans.* **2005**, 3271. (f) Bradley, C. A.; Lobkovsky, E.; Keresztes, I.; Chirik, P. J. *Organometallics* **2006**, *25*, 2080.

(27) Ready, T. E.; Chien, J. C. W.; Rausch, M. D. *J. Organomet. Chem.* **1999**, *583*, 11.

Scheme 1. Copolymerizations with the Functionalized Monomers: (a) Emulsion Polymerization, (b) Partial Silanol Capping, and (c) Further Capping

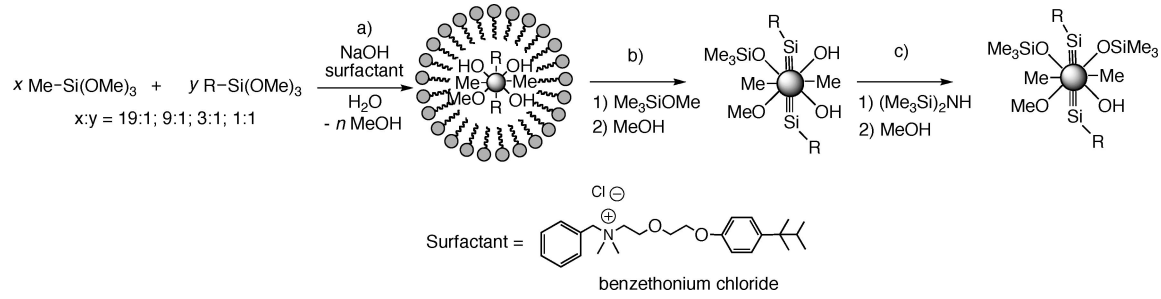

Emulsion Polymerizations with the Functionalized Monomers. All the aforementioned monomers were subjected to conditions previously employed for the generation of polysiloxane nanospheres from $MeSi(OMe)_3$.[17] Neither conventional nor mechanical stirring during these homopolymerizations resulted in tractable products. Typically, gelation and cessation of stirring occurred during the polymerization. In cases where gelation did not occur, a variety of isolation techniques (centrifugation, coprecipitation with other solvents, etc.) were employed, with no success. Also, variations in reaction conditions, including the surfactant to monomer ratio, the solvent level, and the amount of base catalyst added, led to little change in the outcome.

On the basis of the lack of success with homopolymerizations, copolymerizations with methyltrimethoxysilane were attempted with different comonomer weight ratios of 19:1, 9:1, 3:1, and 1:1, using conventional stirring (Scheme 1). This approach was expected to provide polysiloxanes with controlled loadings of functional groups exposed on the nanosphere surface.

In general, the copolymerization strategy proved to be effective for reproducibly providing silicone nanospheres in the desired size regime. The best results were observed for copolymers with low loadings of the functionalized monomer. In certain cases, higher loadings (i.e., 1:1 mixtures or greater) failed to provide nanospheres, as observed for the homopolymerizations. These conditions often result in nonspherical particles with a wide size distribution, as determined by TEM micrographs. This suggests that, in these cases, polymerization occurs outside of the micelle.

A shorthand text notation for the functionalized nanospheres is introduced in Figure 2. This notation identifies the R substituent of the functionalized monomer, neglecting the length of the carbon spacer, as well as the weight ratios of the two silanes. Moreover, the silanol, methoxy, and trimethylsilyl groups represented in the drawings of Figure 2 are omitted for clarity.

Physical Characterization of the Nanospheres. Particle sizes were evaluated by TEM. The TEM micrographs of selected materials (Figure 3) indicate the presence of spherical particles in the 12−28 nm size regime. Particle counts, typically performed on more than 250 nanospheres per sample, and the standard deviations of the functionalized polysiloxanes are compiled in Table 1. Most nanospheres fall within a narrow average diameter of 18−22 nm, and variations in the diameters range between 15 and 25%. Nanospheres containing the indenyl groups consistently gave smaller particles (average diameter = 11 nm for $\mathbf{NS_{Ind}(9:1)}$, 12 nm for $\mathbf{NS_{Ind}(3:1)}$) while the amino-substituted materials gave larger particles (average diameter = 28 nm for $\mathbf{NS_{NH2}(9:1)}$, 26 nm for $\mathbf{NS_{NH2}(3:1)}$). Also, polysiloxanes containing groups that engage in hydrogen bonding tend to exhibit a denser packing of nanospheres (Figure 3b).

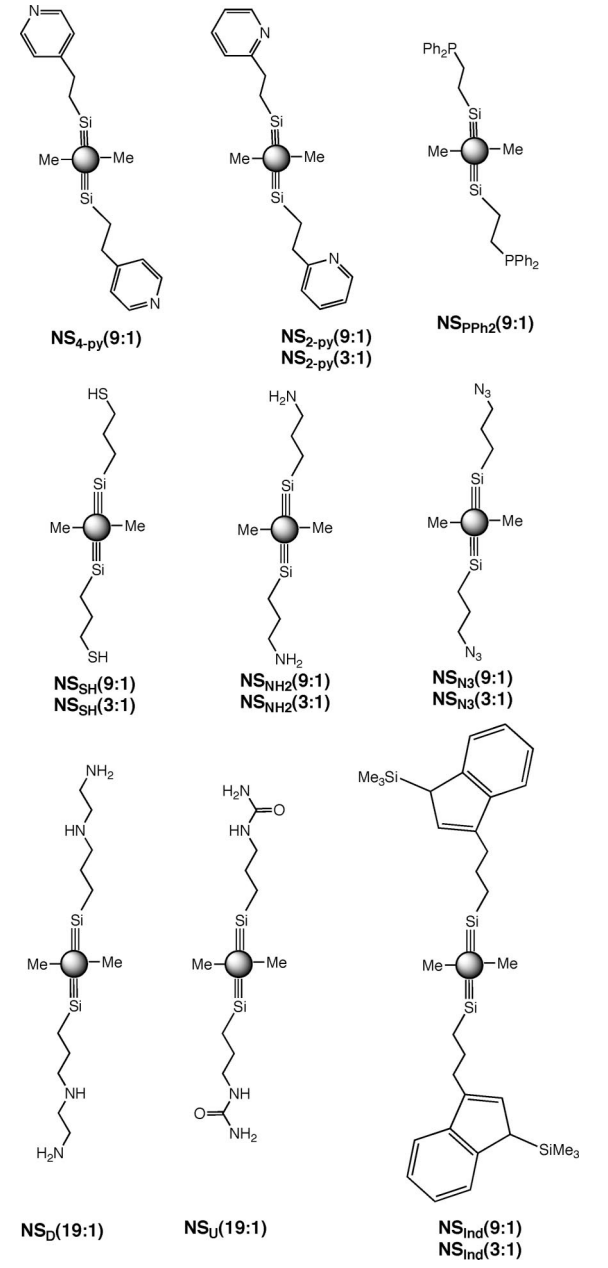

Figure 2. Functionalized copolymer nanospheres along with their shorthand designations.

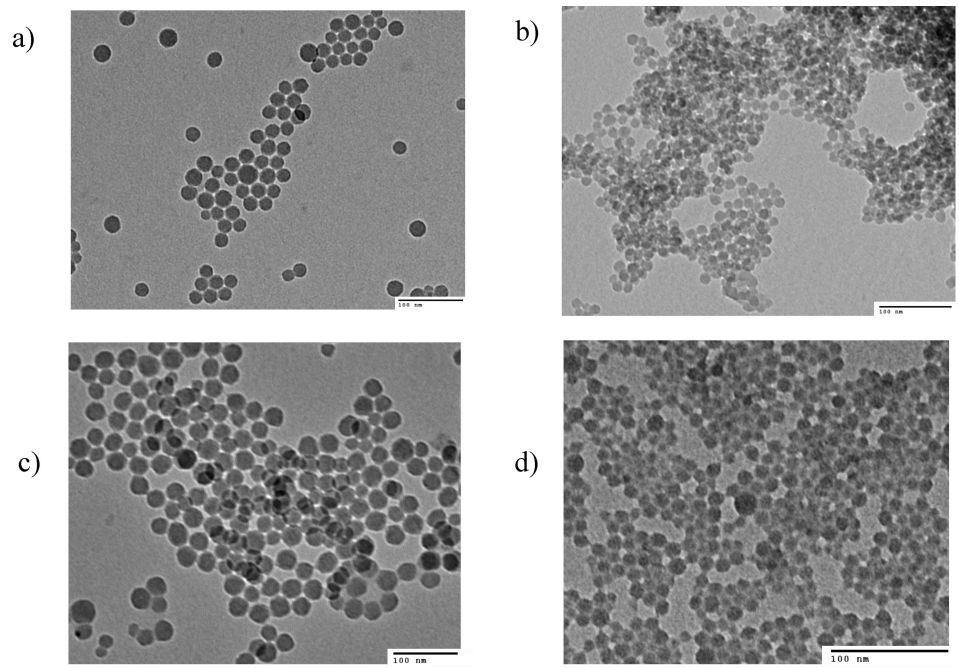

Figure 3. TEM micrographs of selected functionalized nanospheres. (a) **$NS_{4\text{-py}}$(9:1)**, (b) **NS_{D}(19:1)**, (c) **NS_{NH2}(9:1)**, and (d) **NS_{Ind}(9:1)**. Scale bars denote 100 nm.

Table 1. Diameters of the Functionalized Nanospheres based on TEM Microscopy

nanosphere abbreviation	average diameter (nm)	nanosphere abbreviation	average diameter (nm)
$NS_{4\text{-py}}$(9:1)	22(4)	**NS_{NH2}(3:1)**	26(3)
$NS_{2\text{-py}}$(9:1)	20(5)	**NS_{N3}(9:1)**	20(3)
$NS_{2\text{-py}}$(3:1)	19(4)	**NS_{N3}(3:1)**	22(4)
NS_{PPh2}(9:1)	23(4)	**NS_{D}(19:1)**	16(2)
NS_{SH}(9:1)	19(4)	**NS_{U}(19:1)**	19(2)
NS_{SH}(3:1)	21(4)	**NS_{Ind}(9:1)**	11(2)
NS_{NH2}(9:1)	28(3)	**NS_{Ind}(3:1)**	12(2)

TGA/DSC experiments with the nanospheres are consistent with the behavior of hydrophobic materials (see Supporting Information). Thus, in all samples, endothermic water loss is minimal at low temperatures (<150 °C, under dinitrogen) as is the case for many silyl-capped silica-based materials.[28] Sample decomposition, likely due to loss of organic material, normally occurs above 300 °C. The azide-containing nanospheres demonstrate weight losses of 7.3 and 11.4 wt % at temperatures above 200 °C, which is consistent with the elimination of dinitrogen. Similar behavior has been described for poly(glycidyl azide) polymers functionalized with pendant azide groups.[29] A TGA trace of **NS_{PPh2}(9:1)** under dioxygen displays an exothermic weight gain of 3.4% above 120 °C, corresponding to oxidation of surface phosphine groups.

Porosimetry data (Figure 4 and Supporting Information) for the nanospheres at 19:1 and 9:1 comonomer loadings reveal materials with high surface areas, generally displaying type II isotherms. As given in Table 2, BET surface areas typically fall in the 250−300 m^2/g range, as observed for the surface areas of the methyl-functionalized spheres (250−350 m^2/g).[17] The reduced surface areas relative to the methyl nanospheres likely arise from changes in the pore and surface structures with introduction of larger comono-

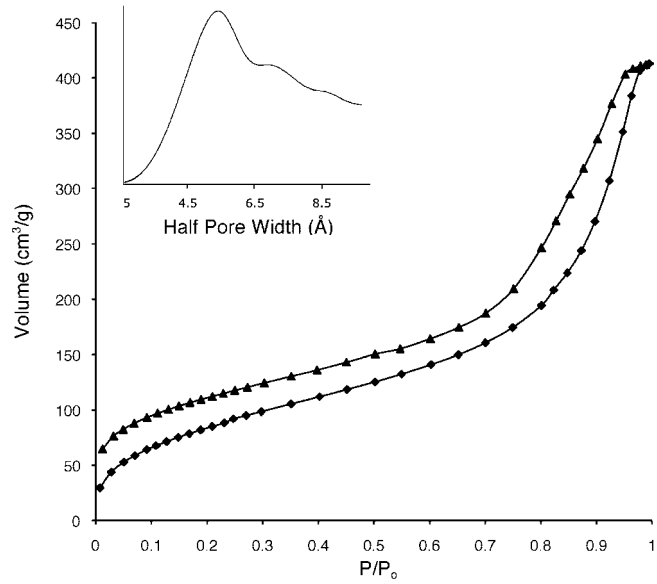

Figure 4. Nitrogen adsorption isotherms, adsorption (◆) and desorption (▲) branches, for **$NS_{4\text{-py}}$(9:1)**. The pore size distribution is shown as an inset.

Table 2. BET Surface Areas and Horvath−Kawazoe Pore Widths for the Functionalized Silicone Nanospheres

nanosphere abbreviation	BET surface area (m^2/g)	H−K pore width (Å)	nanosphere abbreviation	BET surface area (m^2/g)	H−K pore width (Å)
$NS_{4\text{-py}}$(9:1)	323	11	**NS_{N3}(9:1)**	242	11
$NS_{2\text{-py}}$(9:1)	253	11	**NS_{D}(19:1)**	350	11
NS_{PPh2}(9:1)	230	11	**NS_{U}(19:1)**	292	11
NS_{SH}(9:1)	246	11	**NS_{Ind}(9:1)**	293	11
NS_{NH2}(9:1)	310	11			

(28) Brutchey, R. L.; Ruddy, D. A.; Andersen, L. K.; Tilley, T. D. *Langmuir* **2005**, *21*, 9576.
(29) Eroglu, M. S.; Guven, O. *J. App. Polym. Sci.* **1996**, *61*, 201.

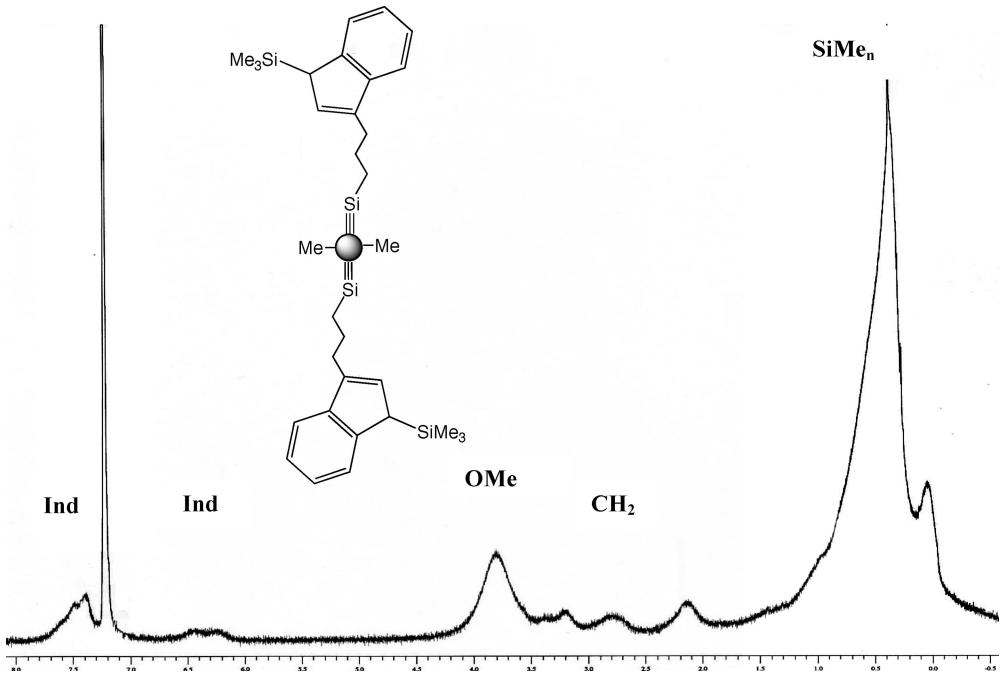

Figure 5. ^{1}H NMR spectrum of **NS$_{Ind}$(9:1)** recorded in benzene-d_6.

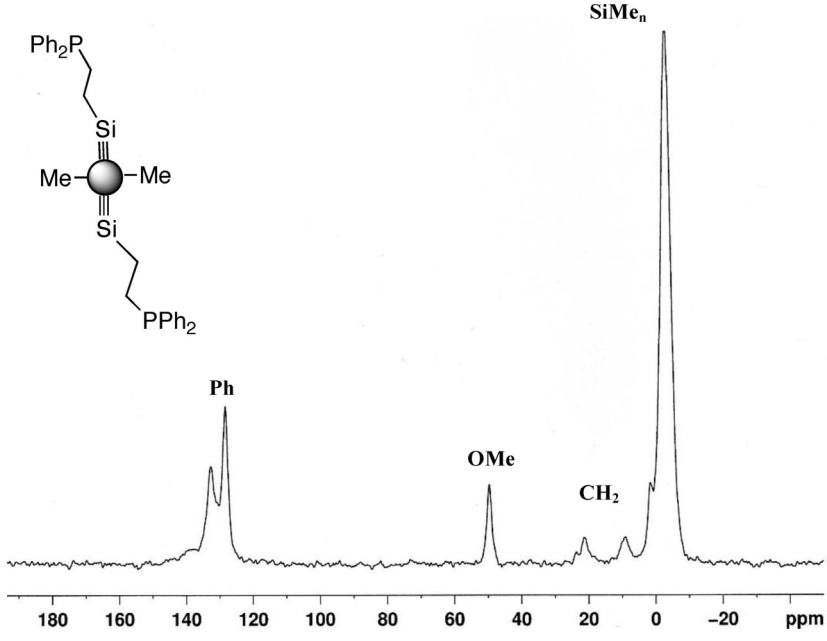

Figure 6. ^{13}C CPMAS spectrum of **NS$_{PPh2}$(9:1)**.

mers. Support for this is provided by micropore analyses (Horvath−Kawazoe method)[30] of the samples, which indicate pores (~11 Å pore widths) that are larger than those observed for the methyl functionalized material (~6 Å pore widths). Porosimetry measurements on the nanospheres at 3:1 comonomer loadings (see Supporting Information) support this assertion, as the surface areas of these materials drop significantly (BET surface areas ranging from 60−140 m^2/g) while pore widths remain fairly constant. Generally, the porosimetry data indicate that the nanospheres with lower loadings of functionalized groups are high surface area materials; hard spheres of similar diameters should have surface areas in the range of 180−200 m^2/g.

As the methyl substituted nanospheres were found to contain residual silanol groups,[17] dibenzyl magnesium titration of the functionalized nanospheres was performed by ^{1}H NMR spectroscopy. From the data of these titrations and with the corresponding surface areas, the SiOH coverages were determined (see Supporting Information).[31] The silanol group densities varied somewhat among the nanospheres examined, but most values fall within a range of 0.5−1.0 OH sites/nm^2. If the silanol groups capped during nanosphere synthesis are accounted for, assuming that approximately 70% are capped as based on reaction of similar functional-

(30) (a) Horvath, G.; Kawazoe, K. *J. Chem. Eng. Jpn.* **1983**, *16*, 470. (b) Sing, K. S. W. *Pure Appl. Chem.* **1985**, *57*, 603. (c) Gregg, S. J.; Sing, K. S. W. *Adsorption, Surface Area and Porosity*; Academic Press: London, 1991.

Table 3. ^{13}C and ^{29}Si CPMAS NMR Data for the Functionalized Silicone Nanospheres[a]

nanosphere	^{13}C Resonances (ppm)				assignment	^{29}Si resonances (ppm)				assignment
$NS_{4\text{-py}}$(9:1)	13.99	28.46			$-CH_2CH_2-$	−66.42	−57.81	−48.96		O_3SiR
	123.21	149.47	153.20		pyridyl	7.78				$OSiMe_3$
$NS_{2\text{-py}}$(9:1)	19.61	37.31			$-CH_2CH_2-$	−66.30	−57.86	−48.68		O_3SiR
	124.90	140.31	152.36	166.23	pyridyl	8.06				$OSiMe_3$
NS_{PPh2}(9:1)	8.98	21.34			$-CH_2CH_2-$	−81.03	−66.18	−57.84		O_3SiR
	128.21	132.58			aryl	8.68				$OSiMe_3$
NS_{SH}(9:1)	1.73	12.45	27.71		$-(CH_2)_3-$	−66.28	−57.40	−50.99	−48.45	O_3SiR
						7.93				$OSiMe_3$
NS_{NH2}(9:1)	1.58	10.77	27.31		$-(CH_2)_3-$	−66.80	−58.22			O_3SiR
						7.79				$OSiMe_3$
NS_{N3}(9:1)	4.25	12.55	25.63		$-(CH_2)_3-$	−66.05	−57.23	−57.02	−48.21	O_3SiR
NS_{Ind}(9:1)	14.04	22.04	27.69	30.97	$-(CH_2)_3-$, CH	−66.43	−57.99	−49.46		O_3SiR
	37.29	44.11				2.85	7.28			$OSiMe_3$
	118.70	124.13	144.31		indene					

[a] $-SiMe_3$ and $-OMe$ ^{13}C resonances, common to all samples, were omitted to focus on the functional group of interest.

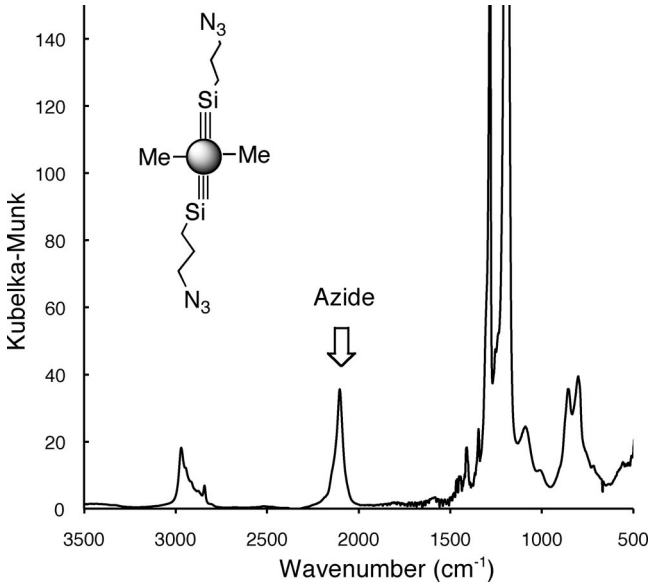

Figure 7. DRIFTS spectrum of **NS_{N3}(3:1)**.

ization agents with unmodified silica,[28] the silanol densities determined for the nanospheres agree well with the number of sites accessible on related SBA15 materials.[28] The presence of SiOH groups is further corroborated by peaks in the 3400−3500 cm^{-1} region in the DRIFTS IR spectra of the materials (see Supporting Information), corresponding to isolated and hydrogen-bonded silanol groups.[28] Thus, these nanoparticles generally contain two types of functional groups—those introduced by the monomers and the silanol groups generated via hydrolysis during the polymerizations.

Characterization of Functional Groups on the Nanospheres. As most of the nanospheres have reasonable solubility in chlorinated and arene solvents, characterization by NMR spectroscopy is possible. In general, the nanospheres exhibit broadened resonances in the regions associated with the corresponding monomer. Figure 5 displays a notable spectrum of **NS_{Ind}(9:1)**, which contains the expected resonances for the silyl indenyl moiety, with methylene hydrogens in the 1−3 ppm region and indenyl protons located in the 6−8 ppm region. The phosphorus NMR spectrum of **NS_{PPh2}(9:1)** in benzene-d_6 (see Supporting Information) exhibits a broad singlet at −8.90 ppm, similar to that of the monomer. Attempts to obtain solution ^{29}Si and ^{13}C NMR spectra of the nanospheres were unsuccessful; in most cases, even with extended collection times, only the methoxy or silyl methyl resonances of the particles were observed. For certain nanospheres, such as **NS_{NH2}(9:1)** or **NS_{NH2}(3:1)**, reduced solubility prevented characterization by solution spectroscopic methods. The decreased solubility of these and related materials likely stems from interparticle hydrogen bonding.

Solid state NMR spectra of the nanospheres (see Supporting Information) are useful, particularly in discerning information about the carbon and silicon environments. The ^{1}H CPMAS NMR spectra typically resemble the corresponding solution spectra. In some cases, line broadening diminishes the peak resolution, especially with resonances in the 1−3 ppm region. Figure 6 displays a representative ^{13}C spectrum, of **NS_{PPh2}(9:1)**. Table 3 compiles pertinent ^{13}C and ^{29}Si solid state NMR data for all the materials. ^{13}C CPMAS NMR spectra display peaks for $SiMe_n$ groups and the methylene carbon spacers in the 0−40 ppm range. Spheres containing aromatic carbons display these characteristic resonances in the 120−160 ppm region. ^{29}Si CPMAS NMR spectra of the materials generally distinguish two major types of silicon environments, those associated with $-OSiMe_3$ caps and those derived from $-O_3SiR$ groups.[32] Several microenvironments exist for both types of Si atoms, based on the degree of monomer condensation. These spectra, coupled with the solution NMR data, provide strong evidence for incorporation of the comonomers into the nanospheres.

Diffuse reflectance UV−visible spectroscopy was also used to characterize the functional groups on the nanospheres (see Supporting Information). For example, **$NS_{2\text{-py}}$(9:1)** and **$NS_{4\text{-py}}$(9:1)** exhibit $\pi-\pi^*$ transitions at 262 and 257 nm, respectively, at nearly the same energies as those associated with the corresponding monomers. The nanospheres **NS_{PPh2}(9:1)**, **NS_{N3}(9:1)**, and **NS_{N3}(3:1)** exhibit electronic transitions at 259, 293, and 293 nm, respectively, which occur at slightly different energies than those of the monomers.

(31) (a) Fujdala, K. L.; Tilley, T. D. *J. Am. Chem. Soc.* **2001**, *123*, 10133. (b) Brutchey, R. L.; Goldberger, J. E.; Koffas, T. S.; Tilley, T. D. *Chem. Mater.* **2003**, *15*, 1040.

(32) Takeuchi, Y.; Takayama, T. In *The Chemistry of Functional Groups: The Chemistry of Organosilicon Compounds*; Patai, S., Rappoport, Z., Apeloig, Y., Eds.; Wiley & Sons: New York, 1998; Vol. II, p 267.

Table 4. Monomer Incorporation Based on Combustion Analyses

nanosphere	% monomer incorporation based on carbon analysis	% monomer incorporation based on heteroatom analysis	functional group density[a] (groups/nm^2)	nanosphere	% monomer incorporation based on carbon analysis	% monomer incorporation based on heteroatom analysis	functional group density[a] (groups/nm^2)
$NS_{4\text{-py}}$(9:1)	60	58	0.71	**NS_{NH2}(3:1)**	56	52	NA
$NS_{2\text{-py}}$(9:1)	66	75	1.05	**NS_{N3}(9:1)**	88	68	1.46
$NS_{2\text{-py}}$(3:1)	54	72	NA	**NS_{N3}(3:1)**	93	71	NA
NS_{PPh2}(9:1)	61	50	0.54	**NS_{D}(19:1)**	65	80	0.89
NS_{SH}(9:1)	90	95	1.80	**NS_{U}(19:1)**	90	85	1.29
NS_{SH}(3:1)	89	92	NA	**NS_{Ind}(9:1)**	25	NA	0.16
NS_{NH2}(9:1)	75	60	1.12	**NS_{Ind}(3:1)**	20	NA	NA

[a] Based on experimentally determined surface areas.

Table 5. EDX Sulfur Analysis of NS_{SH}(3:1)

region	wt % sulfur
1	9.1(0.1)[a]
2	7.7(0.1)[a]
3	8.2(0.1)[a]
4	7.3(0.2)[a]
5	10.8(0.2)[a]
6	7.0(0.2)[a]
average	8.4(1.4)[b]
elementalanalysis	8.49

[a] The values in parenthesis indicate absolute uncertainties of the measurements. [b] The value in parenthesis indicates the standard deviation of the measurements.

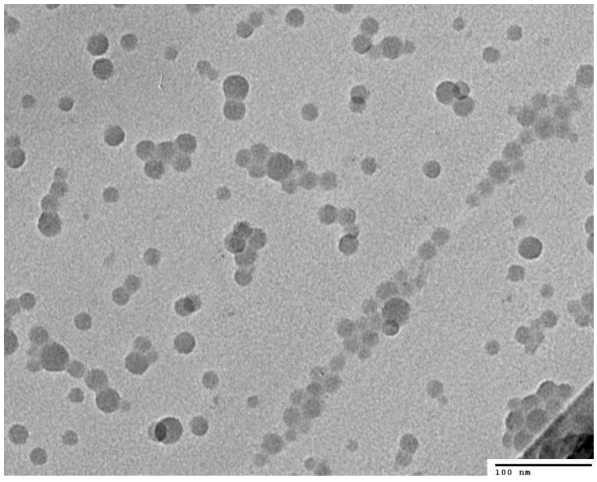

Figure 8. TEM micrograph of **$PdNS_{PPh2}$(9:1)**. The scale bar denotes 100 nm.

DRIFTS measurements were also informative in establishing the presence of the functional groups of interest (see Supporting Information). In most cases, sp^3 C−H stretches for the −CH_2− and −CH_3 groups are observed in the 2900−3000 cm^{-1} region. A sharp band at 2109 cm^{-1} is consistent with stretching of the azide moiety in both **NS_{N3}(9:1)** and **NS_{N3}(3:1)** (Figure 7). The thiol-functionalized spheres, **NS_{SH}(9:1)** and **NS_{SH}(3:1)**, also display distinct SH stretches at 2580 and 2570 cm^{-1}, respectively. Nanospheres containing amino groups, such as **NS_{NH2}(9:1)** and **NS_{D}(19:1)**, exhibit distinctive NH stretches in the 3300−3400 cm^{-1} region. Carbonyl stretches in **NS_{U}(19:1)** appear in the 1550−1700 cm^{-1} region.

As several of the functionalized nanospheres contain heteroatoms, elemental analyses proved to be useful for determination of the comonomer incorporation (Table 4, Supporting Information). In general, 50−60% of the monomer of interest is incorporated into the copolymer nanosphere. Higher incorporations (>70%) are consistently seen

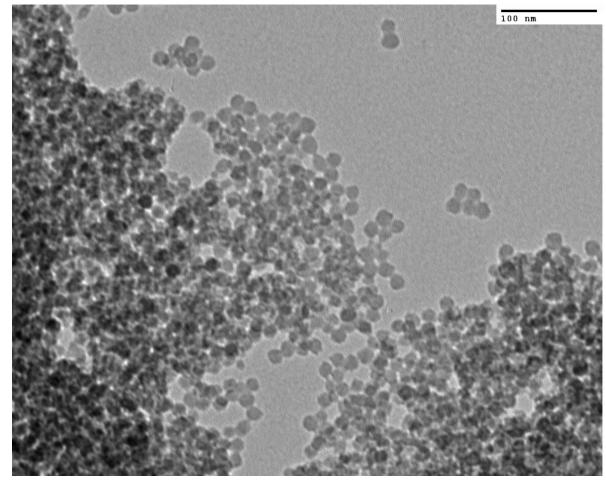

Figure 9. TEM micrograph of **NS_{DU}(18:1:1)**. The scale bar denotes 100 nm.

with the azide and thiol monomers and may result from their greater hydrophobicity,[33] leading to larger effective concentrations of the monomers inside the micelle. The least incorporated group is the silyl indene functionality (∼20% of the expected loading is observed). As shown in Table 4, the % monomer incorporations vary somewhat depending on how they are calculated (on the basis of carbon vs heteroatom analyses). This variation mainly derives from error associated with the heteroatom analysis at these low loading levels.

The amino- and thiol-functionalized spheres were further characterized by titrations using ninhydrin[34] and Ellman's reagent.[35] Quantification of these groups gave loadings of 0.35, 0.30, and 0.58 groups/nm^2, respectively, for **NS_{NH2}(9:1)**, **NS_{D}(19:1)**, and **NS_{SH}(9:1)**. These values are somewhat lower than those determined by combustion analysis, probably due to the inaccessibility of the titration reagent to the micropores of the nanospheres.

Functional Group Dispersity. The chemical and physical properties of the nanospheres should depend, to a great extent, on the dispersities of the functional groups throughout the materials and in particular on the nanosphere surface. Functional group dispersities were determined by energy

(33) For arguments of increased hydrophobicity with low monomer dielectric constant, see Huh, S.; Chen, H.-T.; Wiench, J. W.; Pruski, M.; Lin, V. S.-Y. *J. Am. Chem. Soc.* **2004**, *126*, 1010.

(34) Sarin, V. K.; Kent, S. B. H.; Tam, J. P.; Merrifield, R. B. *Anal. Biochem.* **1981**, *117*, 147.

(35) (a) Ellman, G. L. *Arch. Biochem. Biophys.* **1959**, *82*, 70. (b) Humphrey, R. E.; Ward, M. H.; Hinze, W. *Anal. Chem.* **1970**, *42*, 698.

dispersive X-ray (EDX) spectroscopy.[36] Due to the nature of these experiments, only spheres with heteroatoms could be examined. The quantification of heteroatom content was difficult for nanospheres with lower weight ratios of functionalized monomers, such as **NS_{PPh2}(9:1)**, but reproducible results were obtained for materials containing high weight loadings of sulfur, as in **NS_{SH}(3:1)**.

A representative EDX spectrum, of **NS_{SH}(3:1)**, is shown in the Supporting Information. Scanning procedures involved the use of spot sizes of approximately 18 nm, allowing examination of individual nanospheres or clusters of 2−4 particles. The measured sulfur contents (weight %) for six different regions of **NS_{SH}(3:1)** are listed in Table 5. Note that the average of these values corresponds well with the sulfur content obtained from combustion analysis and reflect a good distribution of functional groups between particles. In an effort to determine variations in functional group dispersity within a single nanosphere, EDX mapping of the surface of an individual particle was attempted by using a smaller spot size (1 nm). However, at this increased intensity of the electron beam, rapid degradation of the particles was observed before reliable quantitative element distributions could be obtained.

Pd Tethering onto the Phosphine Functionalized Nanospheres. As a followup to our previous success with Ti grafting onto silicone nanospheres,[17] attempts were made to employ functional groups on the nanospheres as ligands for other metal centers. Palladium-tethered materials were of particular interest, given the utility of this metal as a catalyst for a wide range of organic transformations.[37] When a toluene or benzene solution of **NS_{PPh2}(9:1)** was exposed to 1 wt % $Pd_2(dba)_3$ (dba = dibenzylideneacetone), a dramatic color change from purple to yellow occurred over the course of 12 h (eq 4). Removal of solvent followed by washing with hexanes gave a yellow powder. Elemental analysis by ICP-OES indicates the presence of 0.87% Pd. Monitoring the reaction by ^{1}H NMR spectroscopy (benzene-d_6 solvent) allowed further characterization of the reaction stoichiometry. These spectra show that addition of $Pd_2(dba)_3$ to **NS_{PPh2}(9:1)** results in elimination of 0.40 (5) equiv of free dba per Pd. The nature of the remaining (dba)Pd-bound species (i.e., mono- versus bimetallic) remains an open question and is difficult to resolve with current characterization techniques. For comparison, the control reaction of $Pd_2(dba)_3$ with unfunctionalized methyl nanospheres results in no reaction, even after heating at 65 °C for 12 h in toluene (based on UV−visible spectroscopy and Pd elemental analyses of the isolated nanospheres following the reaction), demonstrating the necessity of the phosphine groups for reactivity. Moreover, reactions of the phosphine monomer (at several stoichiometries) with $Pd_2(dba)_3$ led to a similar distinct color change, but no products could be isolated from the intractable oils formed upon workup. ^{31}P NMR spectroscopy suggests the presence of multiple products in all cases.

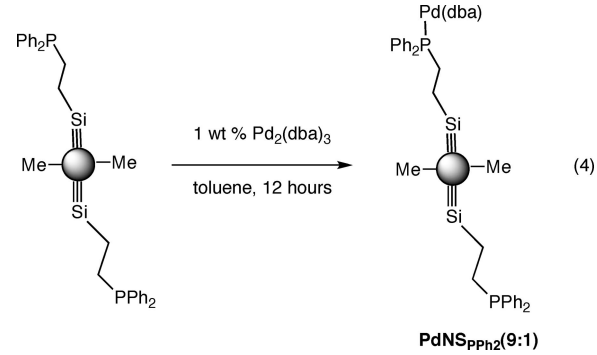

TEM micrographs of **$PdNS_{PPh2}$(9:1)** indicate retention of the spherical morphology, as the particle size remains unchanged (within error) after addition of $Pd_2(dba)_3$ (Figure 8). Moreover, the BET surface area of **$PdNS_{PPh2}$(9:1)** (∼200 m^2/g) is consistent with spherical particles of the expected size (see Supporting Information). Importantly, no bulk Pd nanoparticles are observed. A UV−visible spectrum recorded in acetonitrile (see Supporting Information) indicates retention of the dba unit, with transitions observed at 228 and 318 nm corresponding to the presence of ketone and aryl functionalities much like in the precursor Pd compound. A DRIFTS spectrum (see Supporting Information) of **$PdNS_{PPh2}$(9:1)** demonstrates the presence of dba units and contains C═O stretches in the 1500−1700 cm^{-1} region, which are not seen in **NS_{PPh2}(9:1)**. The presence of Pd(dba) units is also supported by TGA/DSC data (see Supporting Information), which show a loss of 2.3 wt % of **$PdNS_{PPh2}$(9:1)** below 200 °C, in the temperature region where decomposition of $Pd_2(dba)_3$ occurs. For comparison, no weight loss is observed in **NS_{PPh2}(9:1)** until temperatures above 250 °C.

The distribution of Pd throughout the functionalized nanospheres was probed by EDX spectroscopy. Quantification of palladium was not possible, due to the low Pd loading, as ca. 1 wt % borders on the atomic weight percent detection limit of the instrument. Qualitatively, in scanning multiple regions of two independently prepared materials, using spot size diameters of 18 nm, Pd was observed in all areas. This, coupled with the rest of the characterization data, indicates that a Pd molecular precursor can be immobilized on the surface of the phosphine-substituted nansopheres without particle degradation and that the low weight loading allows Pd to be well dispersed throughout the nanoparticles.

Bifunctional Nanospheres. Initial experiments designed to investigate the possible incorporation of multiple functionalities into a single nanosphere targeted the synthesis of polysiloxanes containing amine and ureido groups. A copolymer derived from an 18:1:1 mixture of the monomers methyltrimethoxysilane, *N*-(2-aminoethyl)-3-aminopropyltrimethoxysilane, and ureidopropyltrimethoxysilane was prepared in a manner analogous to that used for other functionalized nanospheres (eq 5). TEM micrographs of **NS_{DU}(18:1:1)** display particles of the expected size, with an average diameter of 17(2) nm (Figure 9). Porosimetry measurements of **NS_{DU}(18:1:1)** indicate a BET surface area of 297 m^2/g. A DRIFTS IR

(36) For general reviews of EDX spectroscopy, see (b) Bando, Y. *J. Elec. Micro.* **1989**, *38*, S81. (a) Krishnan, K. M. *ACS Symp. Ser.* **1989**, *415*, 54.

(37) (a) Wolfe, J. P.; Wagaw, S.; Marcoux, J.-F.; Buchwald, S. L. *Acc. Chem. Res.* **1998**, *31*, 805. (b) Muci, A. R.; Buchwald, S. L. *Top. Curr. Chem.* **2002**, *219*, 131. (c) Buchwald, S. L.; Mauger, C.; Mignani, G.; Scholz, U. *Adv. Synth. Cat.* **2006**, *348*, 23. (d) Hartwig, J. F. *Inorg. Chem.* **2007**, *46*, 1936. (e) Stuart, D. R.; Fagnou, K. *Science* **2007**, *316*, 1172.

Scheme 2. Cooperative Catalysis for Amine and Ureido Groups on a Silica Surface during an Aldol Condensation

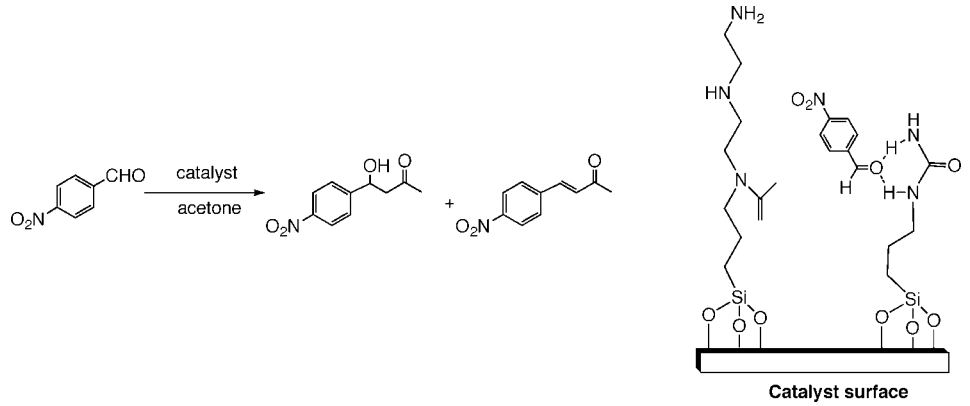

Table 6. Relative Rates for Product Formation in the Nitroaldol Reaction

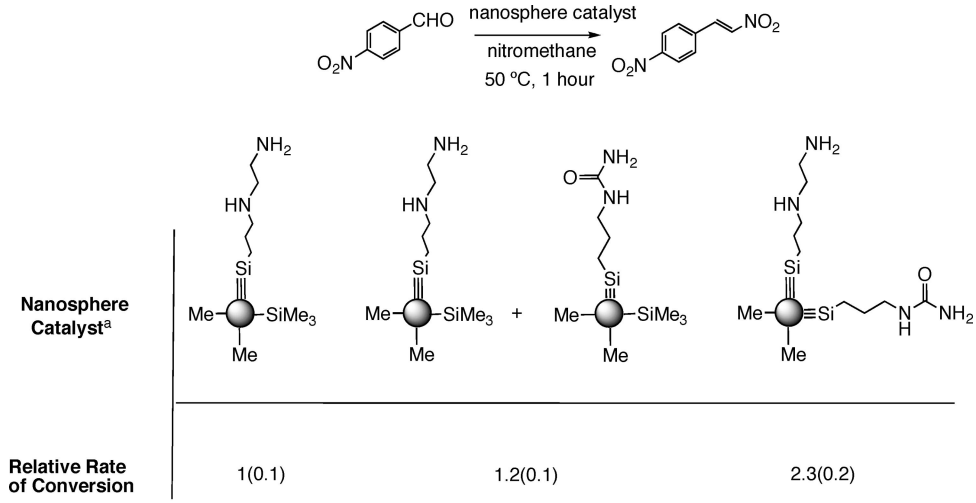

a) all reactions performed with 40 mg of the nanosphere containing diamine functionality.

spectrum of **NS_{DU}(18:1:1)** displays characteristic C═O and NH stretches, while a solid state ^{13}C NMR spectrum of the material confirms the presence of both the carbonyl and CH_2 spacers (see Supporting Information). Titration of the amino groups of **NS_{DU}(18:1:1)** with ninhydrin gave 0.35 amino groups/nm^2, on the basis of the experimental BET surface area, which parallels the amino group loading of **NS_D(19:1)**.

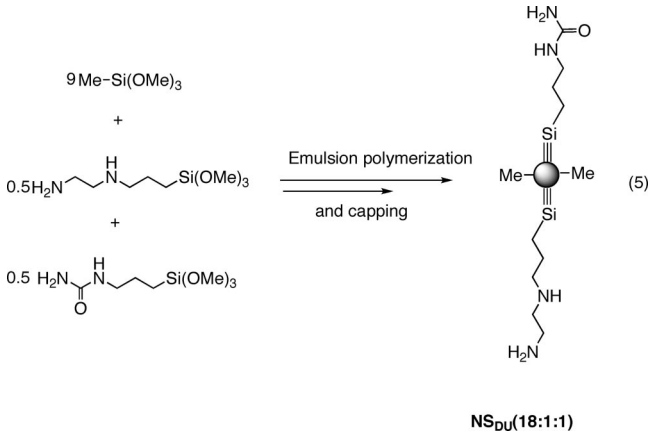

Though physical and chemical evidence points toward retention of the amino and ureido functionalities, they do not provide definitive evidence for incorporation of the two groups onto the same particles. As a probe for the dispersity of the two groups on the surface, experiments were designed to measure any rate enhancement for a base-catalyzed reaction with **NS_{DU}(18:1:1)**. Recently, related rate increases of base-catalyzed reactions by bifunctional silica particles have been used to demonstrate group cooperativity.[38] In these instances, the surface-tethered base is thought to activate the nucleophile while a nearby ureido group hydrogen bonds to the aldehyde substrate, placing it in close proximity to the nucleophile. Apparently, these interactions promote attack and enhance the rate of the reaction (Scheme 2)

The base catalyzed nitroaldol, or Henry, reaction was chosen as the assay for base catalysis with three nanosphere catalysts: **NS_D(19:1)**, an equal weight of **NS_D(19:1)** and **NS_U(19:1)**, and **NS_{DU}(18:1:1)** (Table 6). This reaction was chosen both for its ease of product monitoring as well as the rapid reaction time, which allows for assay of conversion after only 1 h. Conversion was assessed upon workup by ^1H NMR spectroscopy using an internal standard. In general, conversions of 20−50% were observed over 1 h. Control experiments in the absence of any base catalyst consistently gave <5% conversion to the product.

As seen in Table 6, the nanosphere containing both acid and base groups (**NS_{DU}(18:1:1)**) consistently gives a rate enhance-

ment of a factor of 2.3, relative to that of **NS_D(19:1)**. Such rate increases are similar to those observed in related silica-based systems for the same reaction.[38] This result provides evidence for cooperative catalysis and suggests that the functional groups are indeed on the same nanosphere surface. Otherwise, the conversion rates should closely mirror those obtained from mixing the independently prepared nanospheres containing only ureido or diamine groups (**NS_D(19:1)** and **NS_U(19:1)**).

Observation of cooperation between functional groups at these loadings is promising, considering the relatively low weight loadings used in the synthesis of the nanospheres. Moreover, since all three nanospheres used in the catalysis have similar physical properties (i.e., comparable surface areas, average diameters, and approximately equal coverage of amino groups), the observed cooperative effect is likely a function of bringing the two groups in proximity on the nanosphere surface.

Conclusions

This work demonstrates a modular synthesis of high surface area, hydrophobic silicone nanospheres on a 12−28 nm size regime, with well dispersed functional groups, by a simple emulsion copolymerization protocol. A range of functional groups have been incorporated, and the loadings of these groups rival those associated with related silica materials. With phosphino-substituted nanospheres, Pd centers may be anchored on the particle surfaces, without a dramatic change in the physical properties of the support. The inclusion of multiple functional groups on a single particle is also noteworthy, especially since this seems to result in cooperative catalysis of acid and base groups in the nitroaldol reaction. The generality of the emulsion polymerization suggests extension of the current ligand frameworks to incorporate more sophisticated architectures (fluorophores, chelating ligands, etc.), and such possibilities are currently being explored.

Acknowledgment. The authors gratefully acknowledge the support of Wacker Chemie AG and the Director, Office of Energy Research, Office of Basic Energy Sciences, Chemical Sciences Division of the United States Department of Energy under contract DE-AC03-76SF00098. Dr. Michael Lucarelli and Dr. Herbert Barthel (Wacker Chemie AG) are acknowledged for helpful discussions. Ping Yu (UC Davis) and Joseph Ford (Pacific Northwest National Laboratory) are thanked for acquiring solid state ^{1}H, ^{13}C, and ^{29}Si CPMAS data. The Alivisatos group is acknowledged for use of their transmission electron microscope. We also thank the National Center for Electron Microscopy (NCEM) for use of their facilities to acquire EDX spectra.

Supporting Information Available: Additional experimental procedures and spectroscopic data, including TEM micrographs, TGA/DSC data, porosimetry traces, solution and solid state NMR spectra, DRIFTS spectra, DRUV−vis spectra, EDX spectra, and elemental analyses of the nanospheres (PDF). This material is available free of charge via the Internet at http://pubs.acs.org.

CM8018154

(38) (a) Huh, S.; Chen, H.-T.; Wiench, J. W.; Pruski, M.; Lin, V. S.-Y. *Angew. Chem., Int. Ed.* **2005**, *44*, 1826. (b) Zeidan, R. K.; Hwang, S.-J.; Davis, M. E. *Angew. Chem., Int. Ed.* **2006**, *45*, 6332. (c) Margelefsky, E. L.; Zeidan, R. K.; Dufaud, V.; Davis, M. E. *J. Am. Chem. Soc.* **2007**, *129*, 13691. (d) Margelefsky, E. L.; Zeidon, R. K.; Davis, M. E. *Chem. Soc. Rev.* **2008**, *37*, 1118.